

Vessel density in OCT angiography permits differentiation between normal and glaucomatous optic nerve heads

Claudia Lommatzsch¹, Kai Rothaus¹, Joerg Michael Koch¹, Carsten Heinz^{1,2}, Swaantje Grisanti³

¹Department of Ophthalmology, St. Franziskus Hospital, Hohenzollernring 74, Muenster 48145, Germany

²Department of Ophthalmology, University of Essen, Essen 45147, Germany

³Department of Ophthalmology, University of Luebeck, Luebeck 23538, Germany

Correspondence to: Claudia Lommatzsch. Department of Ophthalmology, St. Franziskus Hospital Hohenzollernring 74, Muenster 48145, Germany. claudia.lommatzsch@gmx.de

Received: 2017-10-15 Accepted: 2017-12-01

DOI:10.18240/ijo.2018.05.20

Citation: Lommatzsch C, Rothaus K, Koch JM, Heinz C, Grisanti S. Vessel density in OCT angiography permits differentiation between normal and glaucomatous optic nerve heads. *Int J Ophthalmol* 2018;11(5):835-843

INTRODUCTION

Glaucoma comprises a heterogeneous group of eye diseases. It leads to irreversible loss of ganglion cells and optic neuropathy with typical visual field loss^[1]. Despite the various medical and surgical treatment options, glaucoma is the third most common reason for blindness in the western countries^[2] and the second most common reason worldwide^[3]. With regard to the pathogenesis of the disease, it has long been assumed that mechanical force resulting from increased intraocular pressure (IOP) is exerted on the peripapillary nerve fibers, depressing the fibers and leading to glaucomatous changes (mechanical hypothesis^[4]). The vascular hypothesis, on the other hand, states that perfusion is disturbed by excessive IOP. However, 16% of all people have IOP>22 mm Hg and do not develop any optic nerve damage. These findings indicate that there is a pressure-independent factor. Flammer and Weinreb^[4] proposed that the change in blood flow is part of the cause and not, as long thought, a consequence of the disease. Examination of the ocular vasculature has always been difficult. Many techniques have been devised to measure the hemodynamics of the eye. Due to the specific limitations of each technique, none of them completely satisfied the requirements^[5-6]. With optical coherence tomography angiography (OCTA) it is now possible to assess the blood flow at the optic nerve head (ONH) non-invasively and quantitatively. In 2012, Jia *et al*^[7] were the first to describe measurement of reduced vessel density in glaucomatous eyes by OCTA.

The purpose of our study was to validate the hypothesis of a difference in vessel density (VD) of the ONH between normal and glaucomatous eyes. Furthermore, we investigated the correlations of VD with various structural and functional parameters and rated the accuracy of OCTA in distinguishing between healthy and diseased eyes.

SUBJECTS AND METHODS

In this prospective monocentric study conducted at the

Abstract

• **AIM:** To evaluate whether optical coherence tomography angiography (OCTA) can detect altered vessel density (VD) at the optic nerve head (ONH) in glaucoma patients. Special attention is paid to the accuracy of the OCTA technique for distinguishing healthy from glaucomatous eyes.

• **METHODS:** A total of 171 eyes were examined by the OCTA system AngioVue™ (Optovue): 97 eyes diagnosed with glaucoma and 74 healthy control eyes. The papillary and peripapillary VD was measured. Furthermore, the VD was correlated with different structural and functional measurements. In order to test the accuracy of differentiation between eyes with and without glaucoma, we calculated the receiver operating characteristic curve (ROC) and the area under the curve (AUC).

• **RESULTS:** The papillary and peripapillary VD in glaucomatous eyes was significantly lower than in healthy eyes ($P<0.05$). The VD of the nasal peripapillary sector was significantly lower than in the other sectors. The further the disease had progressed [measured by determining the thickness of the ganglion cell complex (GCC) and the retinal nerve fiber layer (RNFL)] the greater the VD reduction. The AUC discriminated well between glaucomatous and normal eyes (consensus classifier 94.2%).

• **CONCLUSION:** OCTA allows non-invasive quantification of the peripapillary and papillary VD, which is significantly reduced in glaucomatous eyes and accurately distinguishes between healthy and diseased eyes. OCTA expands the spectrum of procedures for detecting and monitoring glaucoma.

• **KEYWORDS:** optical coherence tomography angiography; glaucoma; optic nerve head; blood flow

Department of Ophthalmology, St. Franziskus Hospital Muenster (Germany), data from 97 glaucomatous eyes were evaluated. The healthy control group consisted of 74 eyes. The control subjects were either departmental staff or persons who attended for a routine ophthalmological examination.

The study was approved by the Ethics Committee of the Aerztekammer Westfalen-Lippe, Germany. All patients and volunteers were treated according to stipulations of the Helsinki Declaration and voluntarily participated in the study. Written informed consent was obtained from all participants.

The glaucoma group and the control subjects both had a mean IOP of <21 mm Hg on the day of examination. The participants had no prior history of intraocular surgery, except for cataract extraction, and all were aged >18y. In addition, they all had a refractive error within ± 6 D sphere and ± 2 D cylinder. The control subjects had no family history of glaucoma, a normal appearing ONH, and intact neuroretinal rim and retinal nerve fiber layer (RNFL).

The inclusion criteria for the patient group were the diagnosis of glaucoma and glaucomatous optic neuropathy (cup:disc ratio ≥ 0.5) with corresponding RNFL defects detected by optical coherence tomography (OCT). Exclusion criteria in both groups were significant media opacity preventing high-quality imaging, any ocular disease other than glaucoma or cataract, and previous intraocular operations other than cataract surgery. Persons with systemic hypertension, diabetes, or other vascular diseases such as status post heart failure, apoplexy, or thrombosis were also excluded. In particular, care was taken that no systemic drugs were taken, which could have an effect of vascular diameter either dilation or constriction.

In addition to assessment of the relevant medical history and documentation of the current glaucoma therapy, all participants underwent a comprehensive ocular examination including best-corrected visual acuity testing (BCVA), slit-lamp biomicroscopy, and IOP measurement (Goldmann applanation tonometry), plus visual field examination for the glaucoma patients (mode 30-2, Humphrey Field Analyzer; Zeiss, Jena, Germany). After pupil dilatation with tropicamide 0.5% and phenylephrine hydrochloride 2.5%, the subjects underwent binocular examination of the posterior segment. Subsequently, spectral-domain (SD)-OCT examination of the eye was performed using the OCT System AngioVue™ (RTVue-XR, Optovue, Inc.; Fremont; California, USA; software version 2016.2.035). Prior to the angiography we measured the RNFL, the ganglion cell complex (GCC) thickness, and the rim area at the ONH. The OCTA uses the split-spectrum amplitude-decorrelation angiography algorithm^[8] to capture moving red blood cells. Two volumetric raster scans (one horizontal priority and one vertical priority) were obtained, each with a 4.5 mm×4.5 mm field of view centered on the ONH (302×302 pixels).

Two segmentation levels were considered, designated by the manufacturer as “nerve head” (NH) segmentation (Figure 1A) and “radial peripapillary capillaries (RPC)” segmentation (Figure 1B). The NH segment extends from 2000 μm above the inner limiting membrane (ILM) to 150 μm below the ILM. The RPC segment is a slab from the ILM to the RNFL posterior boundary. All participants underwent SD-OCT and OCTA imaging on the same day. Poor-quality images-defined by a signal strength index (SSI) ≤ 40 were excluded from analysis.

The AngioAnalytics™ software automatically calculates the VD by first extracting a binary image of the vessels from the gray scale of the en-face image and then computing the percentage of pixels of the vessels in the defined sectors or the entire en-face image based on the binary image. Thus, a quotient is formed from the fraction of the pixels with flux perception divided by all the detected pixels. The peripapillary region is defined as a 0.75-mm-wide elliptical annulus. The software calculates the value first as whole vessel density (wVD %) for the ONH and then divides it into an intrapapillary vessel density (iVD) value and an average peripapillary vessel density (pVD) value with further subdivision into six different peripapillary sectors based on the Garway-Heath map (Figure 2).

Statistical Analysis All analyses were performed using MedCalc® Version 12.4 (Ostend, Belgium) and R Version 3.2.5. (Dormagen, Germany). Normal distribution of the data was checked by means of the Kolmogorov-Smirnov test and shown as mean \pm standard deviation (SD; range) for Gaussian distributed values (*t*-test), and average medians (interquartile range) for non-Gaussian distribution (Wilcoxon rank sum test). Correlations were analyzed by Spearman’s rank correlation. To check potential discrimination between glaucomatous and control eyes, a receiver operating characteristics (ROC) curve was used. Moreover, we used Fisher’s linear discriminant analysis (LDA) to find a consensus classifier. LDA is an orthogonal transformation and data reduction technique to minimize intragroup variance and maximize intergroup variance.

RESULTS

The glaucoma group comprised 97 eyes with an average age of 63.17 \pm 12.83y and the control group contained 74 eyes with an average age of 60.78 \pm 15.10y. There were no significant differences in age or refraction (all $P > 0.05$).

With regard to the types of glaucoma, 41 eyes had primary open angle glaucoma (POAG), 26 eyes had pseudoexfoliation (PEX) glaucoma, 24 eyes had normal-tension glaucoma (NTG), and 6 eyes had chronic primary angle-closure glaucoma (CPACG). Further clinical data are presented in Table 1.

As expected, the glaucoma group had lower average values ($P < 0.0001$) for rim area, RNFL, and GCC than the control group (Table 1).

Table 1 Demographics and ocular characteristics of the study population mean±SD; median and interquartile range

Items	Glaucoma group	Control group	P
No. of eyes	97	74	
Age (y)	63.17±12.83	60.78±15.10	0.5
Entity	POAG: 41; PEX: 26; NTG:24; CPACG: 6		
Time since first diagnosis of glaucoma (mo)	91.13±92.58		
Refractive error (D)	-0.44±2.27	-0.05±2.01	0.42
Pseudophakia (n)	32	14	
Cup:disc ratio	0.69±0.18	0.27±0.16	<0.0001
Mean deviation in visual field (dB)	-5.27±7.25		
Antiglaucomatous eye drops (No. of active pharmaceutical ingredients)	2.23±1.49	0	
OCT parameters			
GCC total (μm)	82.49±13.33	97.77±6.4	<0.0001
RNFL average (μm)	77.82±15.33	98.64±9.17	<0.0001
Rim area (mm ²)	0.81 (0.53, 1.07)	1.46 (1.25, 1.59)	<0.0001

POAG: Primary open angle glaucoma; XFG: Exfoliation glaucoma; NTG: Normal-tension glaucoma; CPACG: Chronic primary angle-closure glaucoma; GCC: Ganglion cell complex; RNFL: Retinal nerve fiber layer.

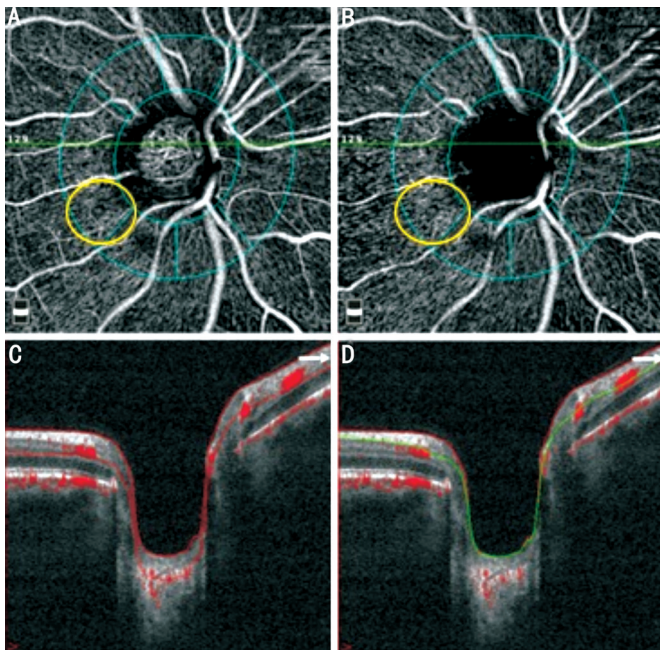


Figure 1 En-face OCT angiography of the ONH segmentation (A), the RPC segmentation (B) and the corresponding B-scan segmentations (C, D) of a right eye.

In both segmentation layers there was a statistically significant difference between glaucomatous and healthy eyes for all results of VD. In all tested sectors, the VD in glaucomatous eyes was significantly lower ($P<0.0001$) than in the control group (Tables 2, 3). Comparing the numerical values of peripapillary VD in both segmentation layers, VD in the RPC layer was significantly higher than in the NH layer. The higher wVD value in the RPC layer is due to a low iVD value, which reduced the total wVD RPC.

On analysis of the clinical findings in the glaucoma group (Table 4), wVD or pVD showed no significant correlation for

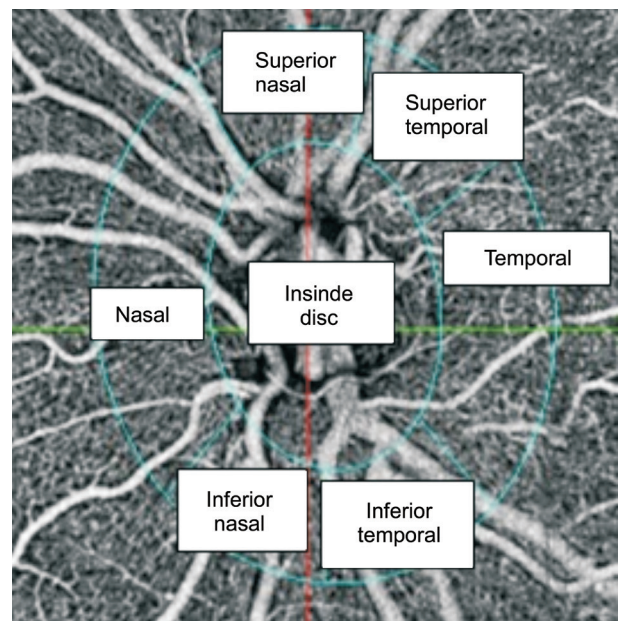


Figure 2 OCTA of the ONH with sector classification of a right eye.

refractive error and IOP. With regard to age, mean deviation in visual field testing, GCC, RNFL, and rim area, however, wVD and pVD were significantly correlated.

There was a strong correlation between the three parameters GCC/RNFL/rim area and wVD/pVD on both segmentation layers. Thinner RNFL, GCC, and rim area were correlated with lower VD (Figures 3, 4).

To check the accuracy of differentiation between eyes with and without glaucoma we calculated the ROC and the area under the curve (AUC). We initially evaluated the following six individual parameters: wVD (RPC/NH), iVD (RPC/NH), and pVD (RPC/NH) (Figure 4). The diagnostic accuracy was best for the iVD in the RPC layer (92.9%), followed by wVD RPC (84.0%),

Table 2 OCTA results for vessel density in the RPC layer mean±SD; median (interquartile range)

Segmentation RPC	Glaucoma group	Control group	P
SSI	54.52±8.97	61.06±11.12	0.009
wVD	46.66 (38.21, 52.35)	54.59 (50.77, 56.01)	<0.0001
iVD	24.0 (16.50, 31.10)	43.29 (38.32, 52.58)	<0.0001
pVD average	57.24 (46.93, 61.11)	61.58 (58.17, 63.85)	<0.0001
pVD nas	53.10 (46.02, 59.07)	58.75 (55.18, 61.68)	<0.0001
pVD infnas	56.30 (45.61, 63.81)	56.30 (45.61, 63.80)	<0.0001
pVD inftemp	58.78 (44.64, 66.26)	66.03 (62.72, 68.55)	<0.0001
pVD suptemp	57.49 (47.57, 68.77)	65.25 (60.83, 68.73)	<0.0001
pVD supnas	51.36±11.01	59.22±5.73	<0.0001
pVD temp	60.66 (51.29, 64.17)	61.12 (58.33, 63.96)	<0.0001

SSI: Signal strength index; RPC: Radial peripapillary capillaries; wVD: Whole vessel density; iVD: Intrapapillary vessel density; pVD: Peripapillary vessel density.

Table 3 OCTA results for vessel density in the NH mean±SD; median (interquartile range)

Segmentation NH	Glaucoma group	Control group	P
SSI	54.52±8.97	61.06±11.12	0.009
wVD	48.62 (41.53, 53.14)	54.28 (50.72, 57.79)	<0.0001
iVD	44.51 (39.02, 49.26)	51.88 (48.18, 57.16)	<0.0001
pVD average	53.97 (45.07, 57.99)	60.25 (56.77, 62.27)	<0.0001
pVD nas	51.35 (44.34, 56.47)	58.68 (55.13, 61.47)	<0.0001
pVD infnas	56.03 (45.36, 61.49)	61.96 (57.42, 65.80)	<0.0001
pVD inftemp	56.72 (44.77, 62.64)	63.97 (60.86, 66.28)	<0.0001
pVD suptemp	54.37 (45.56, 63.64)	63.09 (58.18, 66.24)	<0.0001
pVD supnas	50.73 (39.99, 56.98)	58.67 (53.44, 62.84)	<0.0001
pVD temp	55.71 (44.30, 59.24)	58.30 (54.60, 61.83)	<0.0001

SSI: Signal strength index; NH: Nerve head; wVD: Whole nerve head vessel density; iVD: Intrapapillary vessel density; pVD: Peripapillary vessel density.

Table 4 Spearman correlations between wVD, pVD and clinical parameters

Clinical parameters	wVD RPC (rho/P)	pVD Avg RPC (rho/P)	wVD NH (rho/P)	pVD Avg NH (rho/P)
Refractive error	-0.05/0.65	-0.11/0.3001	-0.03/0.7604	-0.08/0.4202
IOP	0.01/0.96	-0.08/0.4130	-0.02/0.8075	-0.07/0.5044
Age	-0.55/5.88×10 ⁻⁹	-0.51/7.63×10 ⁻⁸	-0.56/2.15×10 ⁻⁹	-0.50/1.08×10 ⁻⁷
MD	0.48/0.0004	0.50/0.0001	0.39/0.0039	0.46/0.00059
GCC total	0.75/1.66×10 ⁻¹⁸	0.72/9.05×10 ⁻¹⁷	0.67/7.33×10 ⁻¹⁴	0.68/1.33×10 ⁻¹⁴
RNFL average	0.81/9.68×10 ⁻²⁴	0.76/1.41×10 ⁻¹⁹	0.72/6.37×10 ⁻¹⁷	0.73/1.99×10 ⁻¹⁷
Rim area	0.70/9.00×10 ⁻¹⁶	0.63/6.89×10 ⁻¹²	0.61/2.60×10 ⁻¹¹	0.64/1.93×10 ⁻¹²

wVD: Whole vessel density; pVD: Peripapillary vessel density; RPC: Radial peripapillary capillaries; NH: Nerve head; IOP: Intraocular pressure; MD: Mean deviation; GCC: Ganglion cell complex; RNFL: Retinal nerve fiber layer; rho: Spearman’s correlation coefficient.

pVD Avg NH (79.4%), wVD NH (78.7%), iVD NH (76.7%), and pVD Avg RPC (74.9%). Moreover, the consensus classifier analyzed using Fisher’s LDA increased the sensitivity and specificity to 94.2%.

To get more detailed results, we increased the number of individual features to 14. Again using Fisher’s LDA as linear classifier, this yielded a 14-dimensional feature vector of 97 glaucomatous and 76 healthy eyes. Table 5 shows the statistics

and performances of the single features and the linear classifier. The P-value was computed using a single-sided t-test. The LDA weights for each single feature were the weighting terms for computing the consensus feature. In the column “AUC ROC” the area under the ROC curve is given. Another characteristic to measure the performance is the true-positive rate (TPR) at a significance level of 5%. In the last column of the table the minimal error number for the classifier is presented.

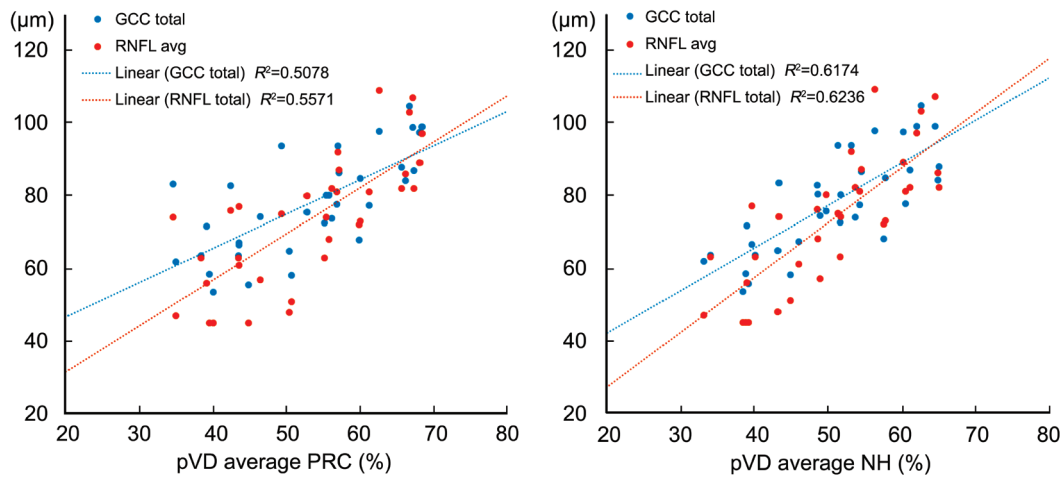


Figure 3 Scatter plots for average pVD and ONH characteristics. A thinner RNFL or GCC correlates significantly with a lower pVD.

Table 5 Linear classifier of 14 dimensional features using Fisher's LDA

Feature	Glaucoma group	Control group	<i>P</i>	LDA weight	AUC ROC (%)	TPR (%) FPR=5%	No. of minimal errors
Consensus	-2.0±1.2	1.3±1.4	9.9×10 ⁻³⁵		95.6	84.5	17
iVD RPC	45.1%±9.3%	23.9%±10.5%	4.5×10 ⁻²⁸	-0.53	92.9	74.2	20
pVD NH inftemp	63.6%±4.1%	54.5%±10.6%	1.4×10 ⁻¹²	0.36	77.8	51.5	45
pVD RPC inftemp	65.4%±4.3%	55.5%±12.4%	1.7×10 ⁻¹¹	-0.38	75.4	50.5	48
pVD RPC supnas	59.2%±5.7%	51.4%±11.0%	9.1×10 ⁻⁹	-0.15	70.9	39.2	54
pVD RPC infnas	62.5%±6.6%	54.3%±11.4%	2.5×10 ⁻⁸	0.23	71.1	38.1	55
pVD NH infnas	61.1%±6.6%	52.9%±10.4%	3.4×10 ⁻⁹	-0.21	74.6	36.1	51
pVD NH supnas	58.2%±6.4%	49.9%±11.0%	3.9×10 ⁻⁹	0.14	72.5	35.1	53
pVD RPC nas	57.9%±5.5%	51.3%±8.9%	1.7×10 ⁻⁸	-0.00	73.5	32.0	51
pVD NH nas	57.6%±5.4%	49.8%±8.6%	2.7×10 ⁻¹¹	-0.24	78.7	32.0	42
pVD NH temp	57.9%±5.5%	52.1%±8.6%	3.2×10 ⁻⁷	-0.17	69.8	28.9	54
iVD NH	51.6%±6.2%	44.7%±6.8%	2.6×10 ⁻¹⁰	0.30	76.7	27.8	47
pVD RPC temp	60.5%±4.6%	56.8%±8.8%	2.7×10 ⁻⁴	0.36	60.1	26.8	66
pVD RPC suptemp	64.0%±6.8%	56.6%±12.3%	9.0×10 ⁻⁷	0.06	68.6	25.8	55
pVD NH suptemp	61.7%±7.3%	54.0%±11.0%	1.3×10 ⁻⁷	0.03	71.7	25.8	50

ROC: Receiver operating characteristic; AUC: Area under curve; LDA: Linear discriminant analysis (Fisher); TPR: True-positive rate; FPR: False-positive rate; iVD: Intrapapillary vessel density; pVD: Peripapillary vessel density; RPC: Radial peripapillary capillaries; NH: Nerve head.

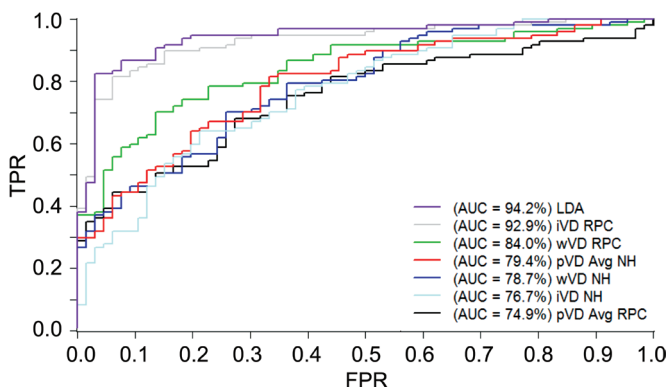


Figure 4 Comparison between whole vessel density, inferior vessel density and peripapillary vessel density in the radial papillary capillaries layer and the nerve head layer in terms of ROC curve, AUC, and in addition, LDA as feature reduction method.

As shown in Table 5 the consensus classifier of the 14 features achieved a good performance for the discrimination of

glaucoma and normal eyes. At a significance level of 5%, a TPR of 84.5% was achieved. The area under the ROC curve was 95.6%. The importance of this classifier for the consensus classifier is confirmed by the highest absolute weight of -0.53 for computing the consensus and lowest *P*-value of the single classifier.

DISCUSSION

In order to better understand the pathogenesis of glaucoma and to investigate the hypothesis of a vascular genesis^[9], the blood circulation of the optic nerve head has been investigated with various examination techniques, including fluorescein angiography^[10-11], laser Doppler flowmetry^[12-13], Heidelberg retina flowmetry^[14], and the Retina Vessel Analyzer^[15]. Since these methods are partly invasive procedures with potential adverse effects^[16] and are also not always available for routine use they have not become established as standard examinations for glaucoma patients.

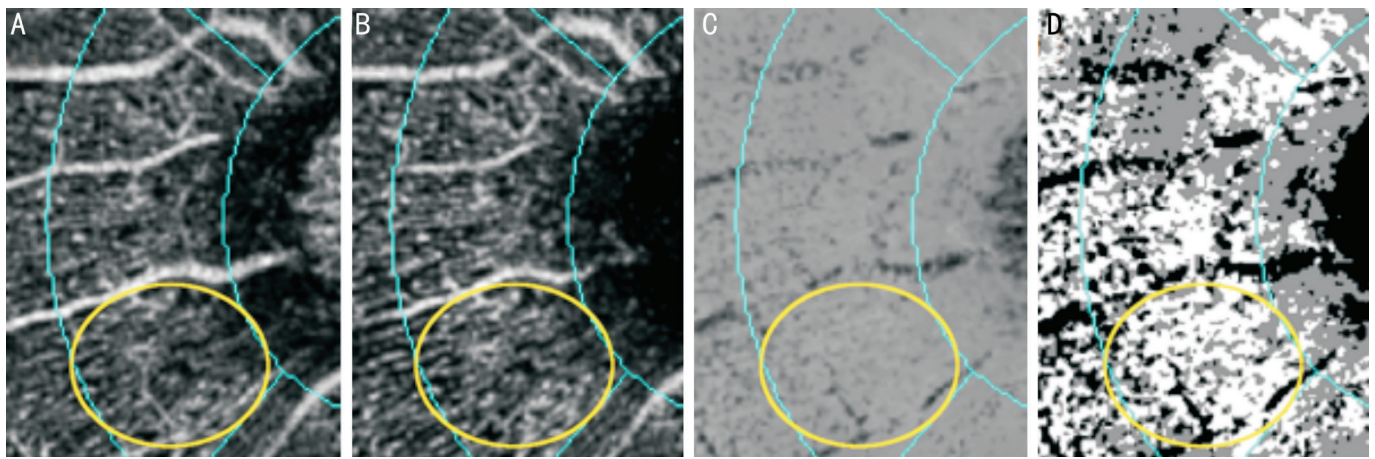


Figure 5 Magnified temporal sector A: NH segmentation; B: RPC segmentation; C: Difference RPC-NH; D: Black pixel: RPC at least 10 gray levels brighter than NH; white pixel: NH at least 10 gray levels brighter than RPC; gray pixel: NH and RPC have same value ± 10 gray levels.

The OCTA with SSADA has great advantages over previous examination methods. It offers non-invasive, high-resolution depiction of the vascular structure in three dimensions. OCTA is not very sensitive to the reflected signal of non-moving tissue and therefore gives a good representation of the individual vessel density^[7]. Taking advantage of light absorption by the erythrocytes, AngioVue™ scans the areas of interest several times. Recording of the moving erythrocytes allows three-dimensional representation of the blood flow and the network of the capillaries in the retina. It supplies scans sized 3 mm×3 mm or 4.5 mm×4.5 mm for the optic nerve. The analysis is presented together with the structural OCT B-scans and the en-face image of the same data set. The details have been described previously^[7].

Since the first description by Jia *et al*^[7] in 2012, there have been numerous publications on this topic. Starting from reports with a low number of cases^[7,17-18], more and more studies are being carried out, confirming in the context of larger numbers of patients that VD is diminished in glaucomatous eyes^[19-21].

In our study we examined a total of 97 glaucomatous eyes. We found that the VD in the radial papillary capillaries layer and in the nerve head layer of glaucomatous eyes was significantly lower than in age-matched control eyes. This is in agreement with our group's earlier study, which, however, had a smaller number of participants^[22]. In contrast to our previous work, this time we measured the VD in six different peripapillary sectors. Clinically, glaucomatous damage occurs predominantly in the temporal superior and temporal inferior sectors of the nerve head and advanced disease leads to nasal shifting of central vessels^[23]. For this reason we had expected the lowest VD in the temporal sector. However, our OCTA results show lower pVD in the nasal and nasal superior ONH sectors compared with the other five sectors (all $P \leq 1.5 \times 10^{-4}$). The VD is also significantly reduced in these two sectors compared with healthy eyes ($P < 0.0001$). If the VD quotient nasal/temporal is formed for both segmentation levels (RPC

and NH), the glaucomatous eyes have a greater reduction of flow than the healthy ones (RPC: $P=0.0002$; NH: $P=0.010$). Differing results have been described in the literature. Jia *et al*^[7] reported a greater reduction of VD in the temporal ONH sector, whereas Rao *et al*^[24] did not find a diminished VD in the temporal sector compared with the entire ONH. We currently have no explanation for the different results; therefore, further investigations are necessary.

Comparing the two segmentation layers, we found higher VD for all of the six peripapillary sectors in the RPC layer. This result is inconsistent with the visual inspection, which suggests higher VD in the NH layer (Figure 5C, 5D). Furthermore, the RPC segmentation is included within the NH segmentation. The average pixel density, however, is slightly higher within the RPC (74.6 vs 73.1; computed using the Fiji software).

A potential explanation for the lower VD in the NH layer is that the en-face image is computed by agglomerating a thicker slice (Figure 1C, 1D). This leads to a lower pixel intensity (=flow) for thin structures (yellow ellipse, Figure 1A, 1B and Figure 5) in the NH layer than in the RPC layer. Computing the flow area, thin structures have a higher contrast on RPC, which gives a more detailed segmentation of the flow area. Thus AngioVue™ computes higher flow area and density, even though physically less flow is agglomerated in the RPC segmentation and both layers (RPC and NH) have the same size.

To obtain a linear correlation between several variables we used the Pearson correlations (Table 4). According to Cohen's classification^[25] neither the IOP nor the refractive error correlated with wVD/pVD. For age and MD we found a moderate correlation with wVD/pVD, while GCC total, RNFL average, and rim area showed a high correlation.

With regard to MD in visual field examination, we had expected a high correlation, as preliminary descriptions showed a significant relationship between wVD/pVD and severity of visual field damage independent of structural loss^[26]. Our results showed only a moderate correlation (Table 4). In the

RPC layer there is a slightly better correlation between VD in OCTA and MD in visual field testing. Comparing our values for the wVD NH layer with the results of Wang *et al*^[27] the results are similar (Wang $r=0.404$ /our study pVD NH $\rho=0.39$). Liu *et al*^[18] demonstrated a stronger correlation of the peripapillary VD with MD, whereby their work was based on a small sample ($n=12$).

With respect to GCC (Wang *et al*^[27] $r=0.4$ /our study $\rho=0.67$) and RNFL (Wang *et al*^[27] $r=0.46$ /our study $\rho=0.72$), Wang *et al*^[27] found a high correlation but the results in our study are even better correlated. However, the correlation values with respect to rim area (Wang *et al*^[27] $r=0.147$ /our study $\rho=0.641$) differ. Lévêque *et al*^[28] also compared ONH perfusion with structural parameters and showed that these were correlated not only with RNFL and GCC but also with rim area. The differing results for correlation with rim area may be explained by different measuring methods. Lévêque *et al*^[28] and our study group measured the rim area automatically with an OCT device, whereas Wang *et al*^[27] do not specify the method used. Furthermore, our study demonstrates that measurement wVD and pVD shows high correlation with the severity of glaucoma, determined by the measurement of the GCC, RNFL, and rim area. This corresponds to recent publications such as that by Chen *et al*^[29]. Some studies have already investigated the diagnostic utility of pVD measured by OCTA, usually compared with the diagnostic utility of the RNFL measured by OCT. Liu *et al*^[18] found that the average pVD and the average thickness of the RNFL have similar sensitivity and specificity. These findings are supported by the results of Yamohammadi *et al*^[30].

By analyzing the VD separately in different sectors and layers of the optic nerve, OCTA adds a valuable diagnostic tool to distinguish a healthy optic nerve from a damaged one. In our study we found that the iVD of the RPC layer has the best diagnostic validity for this purpose (Figure 4). Also, the wVD in both the RPC layer and the NH layer are significantly different in healthy and glaucomatous eyes. Especially the significant difference of the iVD in the RPC layer between control and glaucoma eyes is noticeable. This finding may possibly be explained by the typical excavation form of a glaucomatous ONH. Bayoneting of circumferential vessels occurs in areas where neuroretinal rim tissue has been lost and nasalization of blood vessels occurs in very advanced glaucoma^[23]. The blood vessels run through a glaucomatous ONH with a steep gradient, so that the erythrocytes are moving nearly perpendicular to the OCT optics. This kind of flow cannot be detected reliably by state-of-the-art OCTA devices. Due to these effects the average iVD RPC of glaucoma eyes is not much more than half of the normal density (24.0% in glaucoma eyes vs 43.3% in control eyes; Table 2). Thus, the highest diagnostic accuracy of intrapapillary values could be

an artifact. However, the wVD in the RPC layer, next in the evaluation (Figure 4), also has an excellent accuracy with 84.0%.

In order to examine this observation in more detail, we looked at 14 different parameters using Fisher's LDA. Table 5 shows the statistics and performances of the single features and the linear classifier. All 14 features achieved good performance with regard to discrimination of glaucomatous and normal eyes. Once again, the feature iVD in the RPC layer attained the highest diagnostic value. Standing alone, it was nearly as good as the consensus of all features taken together. The importance of this classifier for the consensus classifier is confirmed by the highest absolute weight of -0.53 for computing the consensus and lowest P -value of the single classifier. No other classifier reached the performance of the iVD feature. Although the P -values are below 0.05, the AUC, the TPR (at 5% significance level) and the minimal error value performed notably worse than the best feature, iVD. Again, it must be critically noted that there may have been measurement error due to the recording technology. However, the inferior temporal pVD, in particular, shows a high degree of accuracy in distinguishing glaucomatous eyes from healthy ones.

Our study has limitations. It does not show whether the diminished VD is the cause or the consequence of the glaucomatous ONH damage. A study by Hollo^[31] showed that peripapillary angioflow density measurements can identify decreased peripapillary perfusion in early glaucoma prior to the development of significant RNFL damage and visual field deterioration. We did not perform any blood pressure measurements during the OCTA scanning. A connection between blood pressure and the ONH blood flow is conceivable. In previous studies, however, no significant correlation between blood pressure and ONH VD was shown^[17-18].

A further limitation is the use of topical glaucoma treatment. Studies using older methods to measure the blood flow under topical medication have yielded varying results. Fuchsjäger-Mayrl *et al*^[32], for example, showed improved blood flow and local carbohydrate inhibitors, whereas Pillunat *et al*^[33] did not demonstrate any change. Takusagawa *et al*^[34] even found an association between β -blocker eyedrop use and decreased macular VD in glaucomatous eyes measured by OCTA. Ninety-two percent of our glaucoma patients were using IOP-lowering eyedrops, and for ethical and medical reasons we did not discontinue the local medication before the study.

Furthermore, a limitation on the use of phenylephrine for pupil dilation has to be discussed. It is a selective α_1 -adrenergic receptor agonist with vasoconstrictive effect. In a study by Vandewalle *et al*^[35] however, it has been shown that addition of phenylephrine (in this work even at 5% concentration) to tropicamide 0.5% does not influence retinal vessel diameter in

glaucoma patients. Nevertheless should avoid using vasoactive substances in future work whenever possible.

Our work demonstrates that spectral domain OCTA can measure reduced vessel density at the optic nerve head in glaucomatous eyes and that these findings are correlated to functional and structural glaucomatous alterations. In addition, the further the disease has advanced, the more the vessel density is reduced. To the best of our knowledge, there are currently no similar studies investigating the possibility of distinguishing between healthy and glaucomatous eyes in detail. On the basis of 14 different features it was shown that the OCTA technique is able to distinguish glaucomatous from healthy eyes with high reliability.

ACKNOWLEDGEMENTS

Conflicts of Interest: Lommatzsch C, lecture Optovue; Rothaus K, None; Koch JM, None; Heinz C, None; Grisanti S, None.

REFERENCES

- Weinreb RN, Khaw PT. Primary open-angle glaucoma. *Lancet* 2004;363(9422):1711-1720.
- Dietlein TS, Hermann MM, Jordan JF. The medical and surgical treatment of glaucoma. *Dtsch Arztebl Int* 2009;106(37):597-605.
- Resnikoff S, Pascolini D, Etya'ale D, Kocur I, Pararajasegaram R, Pokharel GP, Mariotti SP. Global data on visual impairment in the year 2002. *Bull World Health Organ* 2004;82(11):844-851.
- Fechtner RD, Weinreb RN. Mechanisms of optic nerve damage in primary open angle glaucoma. *Surv Ophthalmol* 1994;39(1):23-42.
- Harris A, Chung HS, Ciulla TA, Kagemann L. Progress in measurement of ocular blood flow and relevance to our understanding of glaucoma and age-related macular degeneration. *Prog Retin Eye Res* 1999;18(5):669-687.
- Schuman JS. Measuring blood flow: so what? *JAMA Ophthalmol* 2015;133(9):1052-1053.
- Jia Y, Morrison JC, Tokayer J, Tan O, Lombardi L, Baumann B, Lu CD, Choi W, Fujimoto JG, Huang D. Quantitative OCT angiography of optic nerve head blood flow. *Biomed Opt Express* 2012;3(12):3127-3137.
- Jia Y, Tan O, Tokayer J, Potsaid B, Wang Y, Liu JJ, Kraus MF, Subhash H, Fujimoto JG, Hornegger J, Huang D. Split-spectrum amplitude-decorrelation angiography with optical coherence tomography. *Opt Express* 2012;20(4):4710-4725.
- Flammer J, Orgül S, Costa VP, Orzalesi N, Krieglstein GK, Serra LM, Renard J-P, Stefánsson E. The impact of ocular blood flow in glaucoma. *Prog Retin Eye Res* 2002;21(4):359-393.
- Arend O, Plange N, Sponsel WE, Remky A. Pathogenetic aspects of the glaucomatous optic neuropathy: fluorescein angiographic findings in patients with primary open angle glaucoma. *Brain Res Bull* 2004;62(6):517-524.
- Talusan E, Schwartz B. Specificity of fluorescein angiographic defects of the optic disc in glaucoma. *Arch Ophthalmol* 1977;95(12):2166-2175.
- Piltz-seymour JR, Grunwald JE, Hariprasad SM, Dupont J. Optic nerve blood flow is diminished in eyes of primary open-angle glaucoma suspects. *Am J Ophthalmol* 2001;132(1):63-69.
- Hamard P, Hamard H, Dufaux J, Quesnot S. Optic nerve head blood flow using a laser Doppler velocimeter and haemorheology in primary open angle glaucoma and normal pressure glaucoma. *Br J Ophthalmol* 1994;78(6):449-453.
- Logan JFJ, Rankin SJA, Jackson AJ. Retinal blood flow measurements and neuroretinal rim damage in glaucoma. *Br J Ophthalmol* 2004;88(8):1049-1054.
- Ramm L, Jentsch S, Peters S, Augsten R, Hammer M. Investigation of blood flow regulation and oxygen saturation of the retinal vessels in primary open-angle glaucoma. *Graefes Arch Clin Exp Ophthalmol* 2014;252(11):1803-1810.
- Stein MR, Parker CW. Reactions following intravenous fluorescein. *Am J Ophthalmol* 1971;72(5):861-868.
- Jia Y, Wei E, Wang X, Zhang X, Morrison JC, Parikh M, Lombardi LH, Gattley DM, Armour RL, Edmunds B, Kraus MF, Fujimoto JG, Huang D. Optical coherence tomography angiography of optic disc perfusion in glaucoma. *Ophthalmology* 2014;121(7):1322-1332.
- Liu L, Jia Y, Takusagawa HL, Pechauer AD, Edmunds B, Lombardi L, Davis E, Morrison JC, Huang D. Optical coherence tomography angiography of the peripapillary retina in glaucoma. *JAMA Ophthalmol* 2015;133(9):1045-1052.
- Shin JW, Lee J, Kwon J, Choi J, Kook MS. Regional vascular density-visual field sensitivity relationship in glaucoma according to disease severity. *Br J Ophthalmol* 2017;101(12):1666-1672.
- Rao HL, Kadambi SV, Weinreb RN, Puttaiah NK, Pradhan ZS, Rao DAS, Kumar RS, Webers CAB, Shetty R. Diagnostic ability of peripapillary vessel density measurements of optical coherence tomography angiography in primary open-angle and angle-closure glaucoma. *Br J Ophthalmol* 2017;101(8):1066-1070.
- Suh MH, Zangwill LM, Manalastas PI, Belghith A, Yarmohammadi A, Medeiros FA, Diniz-Filho A, Saunders LJ, Yousefi S, Weinreb RN. Optical coherence tomography angiography vessel density in glaucomatous eyes with focal lamina cribrosa defects. *Ophthalmology* 2016;123(11):2309-2317.
- Lommatzsch C, Koch JM, Claußnitzer H, Heinz C. OCT angiography of the glaucoma optic nerve. *Klin Monbl Augenheilkd* 2018;235(2):205-211.
- Gandhi M, Dubey S. Evaluation of the optic nerve head in glaucoma. *J Curr Glaucoma Pract* 2013;7(3):106-114.
- Rao HL, Pradhan ZS, Weinreb RN, Reddy HB, Riyazuddin M, Dasari S, Palakurthy M, Puttaiah NK, Rao DA, Webers CA. Regional comparisons of optical coherence tomography angiography vessel density in primary open-angle glaucoma. *Am J Ophthalmol* 2016;171:75-83.
- Cohen J. *Statistical Power Analysis for the Behavioral Sciences*. 2. edition. Hillsdale: Lawrence Erlbaum Associates; 1988.
- Yarmohammadi A, Zangwill LM, Diniz-Filho A, Suh MH, Yousefi S, Saunders LJ, Belghith A, Manalastas PI, Medeiros FA, Weinreb RN. Relationship between optical coherence tomography angiography vessel density and severity of visual field loss in glaucoma. *Ophthalmology* 2016;123(12):2498-2508.

- 27 Wang X, Jiang C, Ko T, Kong X, Yu X, Min W, Shi G, Sun X. Correlation between optic disc perfusion and glaucomatous severity in patients with open-angle glaucoma: an optical coherence tomography angiography study. *Graefes Arch Clin Exp Ophthalmol* 2015;253(9):1557-1564.
- 28 Lévêque PM, Zéboulon P, Brasnu E, Baudouin C, Labbé A. Optic disc vascularization in glaucoma: value of spectral-domain optical coherence tomography angiography. *J Ophthalmol* 2016;2016:6956717.
- 29 Chen CL, Bojikian KD, Gupta D, Wen JC, Zhang Q, Xin C, Kono R, Mudumbai RC, Johnstone MA, Chen PP, Wang RK. Optic nerve head perfusion in normal eyes and eyes with glaucoma using optical coherence tomography-based microangiography. *Quant Imaging Med Surg* 2016;6(2):125-133.
- 30 Yarmohammadi A, Zangwill LM, Diniz-Filho A, Suh MH, Manalastas PI, Fatehee N, Yousefi S, Belghith A, Saunders LJ, Medeiros FA, Huang D, Weinreb RN. Optical coherence tomography angiography vessel density in healthy, glaucoma suspect, and glaucoma eyes. *Invest Ophthalmol Vis Sci* 2016;57(9):OCT451-459.
- 31 Holló G. Vessel density calculated from OCT angiography in 3 peripapillary sectors in normal, ocular hypertensive, and glaucoma eyes. *Eur J Ophthalmol* 2016;26(3):e42-e45.
- 32 Fuchsjäger-Mayrl G, Wally B, Rainer G, Buehl W, Aggermann T, Kolodjaschna J, Weigert G, Polska E, Eichler HG, Vass C, Schmetterer L. Effect of dorzolamide and timolol on ocular blood flow in patients with primary open angle glaucoma and ocular hypertension. *Br J Ophthalmol* 2005;89(10):1293-1297.
- 33 Pillunat LE, Böhm AG, Köller AU, Schmidt KG, Klemm M, Richard G. Effect of topical dorzolamide on optic nerve head blood flow. *Graefes Arch Clin Exp Ophthalmol* 1999;237:495-500.
- 34 Takusagawa HL, Liu L, Ma KN, Jia Y, Gao SS, Zhang M, Edmunds B, Parikh M, Tehrani S, Morrison JC, Huang D. Projection-resolved optical coherence tomography angiography of macular retinal circulation in glaucoma. *Ophthalmology* 2017;124(11):1589-1599.
- 35 Vandewalle E, Abegão Pinto L, Olafsdottir OB, Stalmans I. Phenylephrine 5% added to tropicamide 0.5% eye drops does not influence retinal oxygen saturation values or retinal vessel diameter in glaucoma patients. *Acta Ophthalmol* 2013;91(8):733-737.